Methane Decarbonization in Indirect Heating Solar Reactors of 20 and 50 kW for a CO2-Free Production of Hydrogen and Carbon Black

Sylvain Rodat, Stéphane Abanades, Gilles Flamant

J_ID: SLE DOI: 10.1115/1.4004238 Date: 25-May-11 Stage: Page: 1 Total Pages: 8

Methane Decarbonization in Indirect Heating Solar Reactors of 20 and 50 kW for a CO_2-Free Production of Hydrogen and Carbon Black

Sylvain Rodat

Stéphane Abanades[1]
e-mail: stephane.abanades@promes.cnrs.fr

Gilles Flamant

Processes, Materials, and
Solar Energy Laboratory,
PROMES-CNRS,
7 Rue du Four Solaire,
66120 Font-Romeu, France

Solar methane decarbonization is an attractive pathway for a transition toward an hydrogen-based economy. In the frame of the European SOLHYCARB project, it was proposed to investigate this solar process extensively. At CNRS-PROMES, two indirect heating solar reactors (20 and 50 kW) were designed, built, and tested for methane decarbonization. They consist of graphite cavity-type receivers approaching the blackbody behavior. The CH_4 dissociation reaction was carried out in tubular sections inserted in the solar absorber receiving concentrated solar irradiation. The 20 kW solar reactor (SR20) was especially suitable to study the chemical reaction and methane conversion performances depending on the experimental conditions (mainly temperature and residence time). The 50 kW solar reactor (SR50) was operated to produce significant amounts of carbon black for determining its properties and quality in the various possible commercial applications. The main encountered problem concerned is the particle evacuation. Solutions were proposed for large-scale industrial applications. A process analysis was achieved for a 14.6 MW solar chemical plant on the basis of a process flow-sheet. A production of 436 kg/h of hydrogen and 1300 kg/h of carbon black could be obtained for 1737 kg/h of methane consumed, with an hydrogen cost competitive to conventional methane reforming. This paper summarizes the main results and conclusions of the project.
[DOI: 10.1115/1.4004238]

Keywords: hydrogen, carbon black, solar reactor, pilot scale, methane decomposition, cracking

1 Introduction

Hydrogen is viewed as a potential energy carrier for the future, [1] but it is not available in nature and it must be extracted from available sources (fossil fuels, biomass, or water). Carbon black (CB) has many industrial application fields related to their key properties such as in rubbers reinforcing (mechanical properties), inks (pigment properties), and conductive polymers (electrical properties), etc. [2]. Today, applications in tire and rubber product manufacturing industry represent 90% of world carbon black production [3]. The total world CB production is about 8 Mt/yr and the selling price depends on the product nanostructure. It may vary from 0.6 €/kg for standard CB to 3 €/kg for high-grade conductive CB. In contrast to classical soot that always contains a lot of inorganic contaminants and extractable organic residues, commercial CB contains mainly elemental carbon (97–99%) depending on the manufacturing process [2]. At present, more than 90% of the CB is produced by incomplete combustion processes and the remaining part by thermal decomposition of hydrocarbons, depending upon the presence or absence of oxygen. In the furnace process, CB is produced by combustion of oil (feedstock) in a natural gas flame [4]. The steam-methane reforming and the furnace process (incomplete combustion of hydrocarbons in air) are the conventional production processes of hydrogen and CB, respectively. However, they release large amounts of CO_2 in the atmosphere. CO_2 sequestration is limited and new technologies have to be investigated [5]. Consequently, it is necessary to think about sustainable ways of production. Current processes for H_2 and CB production are performed at an industrial scale but are not combined. Moreover, the process heat is supplied by burning a significant portion of the feedstock. Solar methane dissociation thus appears as an attractive step toward an hydrogen-based economy [6]. It takes advantage of the co-production of hydrogen and CB without fossil fuel combustion for energy supply. The use of solar energy for processing heat avoids both gaseous products contamination and pollutants emission (e.g., CO, CO_2, NO_x, SO_x). Actually, this solar route avoids energy consumption and pollution associated with both H_2 and CB production by classical methods. Quantitatively, it was estimated that the solar-thermal process saves 277 MJ of fossil fuel and avoids 13.9 kg-equivalent CO_2 per kg of H_2 produced in comparison to conventional steam-methane reforming and furnace black processing [7]. CB can be sold on the market, thereby leading to a possible competitive process for hydrogen production. Alternatively, CB can also be safely stored keeping a value in terms of CO_2 credits. The targeted applications for the solar produced CB concern polymer composites (rubber and plastics) and primary and secondary batteries. Methane decomposition is a topic of growing interest in research centers. Numerous reactor configurations have been studied at laboratory scale (up to 5 kW): direct [8,9] or indirect [10,11] heating reactors (tubular or vortex type), catalytic [12–14], or noncatalytic [15] reactions. The process is now ready for preindustrial tests. Industrial patents were also applied [16,17]. Regarding the economics of the process, the valorization of both products (i.e., hydrogen and CB) is of primary importance [7]. Therefore, not only the

[1]Corresponding author.

Contributed by the Solar Energy Division of ASME for publication in the JOURNAL OF SOLAR ENERGY ENGINEERING. Manuscript received December 14, 2010; final manuscript received April 15, 2011; published online xx xx, xxxx. Assoc. Editor: Tatsuya Kodama.

chemical conversion has to be investigated but also the CB properties. The reactors developed previously involved usually a flow of CH_4 laden with fine carbon particles *that serve simultaneously as radiant absorbers and nucleation sites for the heterogeneous decomposition reaction. Thus, such a route subjected to carbon particle addition pertains to the* thermocatalytic decomposition of methane *since these added carbon particles may act as reaction catalysts.* The following work presents the performances assessment of two solar reactors developed for methane splitting at 20 and 50 kW scales without any addition of carbon material in the reactor. Both hydrogen and CB productions are discussed in terms of chemical conversion and CB quality.

2 Experimental Set-up of Solar Reactors SR20 and SR50

2.1 Reactor Designs. Two solar reactors were designed, built, and tested. Both of them are based on the concept of indirect heating reactors, i.e., the solar irradiated zone is separated from the reacting flow, and thus particles deposition on the optical window cannot occur. They are approaching the blackbody behavior, thanks to a graphite cavity absorber with a small aperture. These cavities are insulated and inserted in a metallic box equipped with a water-cooled front face. The reactors are lined with several insulating layers surrounding the graphite cavity (total thickness of 15 cm) to reduce thermal losses. The insulating materials are carbon felt as a first layer in contact with the graphite cavity ($\lambda = 0.46$ W m^{-1} K^{-1}), an intermediate refractory ceramic fibers resistant up to 1600 °C (62% Al_2O_3, 30% SiO_2, $\rho = 200$ kg/m^3, $\lambda = 0.25$ W m^{-1} K^{-1} at 1200 °C, $\lambda = 0.35$ W m^{-1} K^{-1} at 1400 °C, $\lambda = 0.48$ W m^{-1} K^{-1} at 1600 °C) and an outer layer of a very efficient microporous insulator operating up to 1000 °C (20% ZrO_2, 77.5% SiO_2, 2.5% CaO, $\rho = 300$ kg/m^3, $\lambda = 0.044$ W m^{-1} K^{-1} at 800 °C). A transparent hemispherical quartz window prevents the cavity oxidation. SR20 is presented in Fig. 1. The cavity is of cubic shape (20 cm-side). It is crossed by four independent vertical graphite tubes and has an aperture diameter of 9 cm. The tubes are equally separated and placed at about 2.5 cm from the backside of the cavity. Each reaction zone is composed of two concentric graphite tubes. The gas enters the inner tube and flows out by the annular space between the outer and inner tubes. This design permits to increase the gas residence time and to preheat the reactants. The inner tube diameters are 12 mm o.d. and 4 mm i.d. The outer tube diameters are 24 mm o.d. and 18 mm i.d. More details can be found elsewhere [18,19].

The 50 kW solar reactor is displayed in Fig. 2. It is twice the size of SR20. The reactor body is made of an aluminum shell (800 mm × 780 mm × 505 mm) and a water-cooled front face with a 13 cm-diameter aperture to let concentrated solar radiation entering within the reactor cavity. The graphite cavity side is about 40 cm and it is crossed by seven horizontal graphite tubes (800 mm length, 26 mm o.d., 18 mm i.d.). Additional information can be read in Ref. [20].

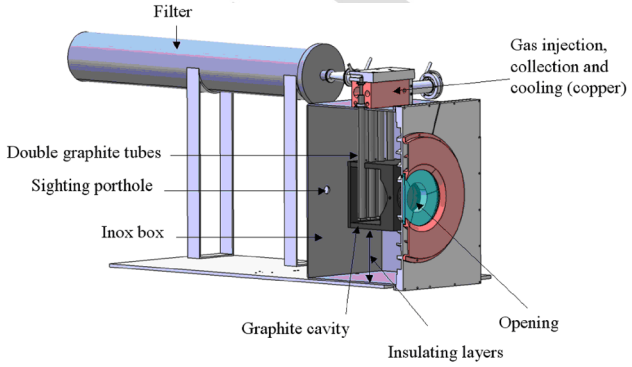

Fig. 1 Scheme of the 20 kW solar reactor

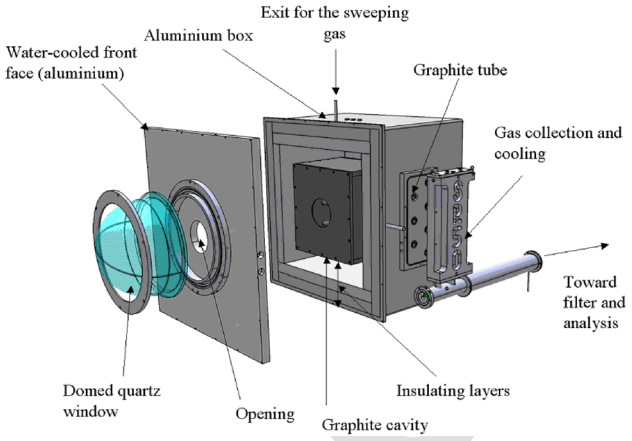

Fig. 2 Scheme of the 50 kW solar reactor

2.2 Experimental Methods. For both reactors, the first experimental step was the heating of the reactor with an argon flow in the tubes. Once the desired temperature has reached, the mixture of argon and methane was injected with a controlled composition. Two mass-flow meters were dedicated to each tube to control accurately the Ar and CH_4 flow-rates. The temperature was measured by a solar blind optical pyrometer (wavelength: 5.14 μm) pointing toward the outer wall of a graphite tube inside the cavity through a lateral fluorine (CaF_2) window. Pt–Rh thermocouples were also used. Temperatures at various locations (especially in the insulation zone against the cavity wall) were monitored and recorded continuously. At the exit of each tube, the exhaust gas-solid flows were collected, cooled, and mixed together. The solid and gaseous products were cooled down and flowed through a filter bag to separate carbon particles. The pressure was monitored by pressure sensors placed at each tube entrance and was regulated thanks to the use of a Venturi vacuum pump (absolute operating pressure of about 40 kPa). The filtered gas was then analyzed online to determine the gas composition during the progress of the reaction. A continuous analyzer permitted to monitor the concentration of H_2 and CH_4. The methods used for H_2 and CH_4 analysis were thermal conductivity and non-dispersive infrared detections, respectively. A gas chromatograph also measured online the outlet concentrations of CH_4, C_2H_6, C_2H_4, C_2H_2, and H_2. The chromatograph (Varian CP 4900) was equipped with two columns: MolSieve 5A PLOT calibrated for H_2 and CH_4 and PoraPLOT U calibrated for light hydrocarbons (C_2H_y). The chromatography analysis was based on thermal conductivity detection and the carrier gas was argon, also used as buffer gas during methane cracking experiments, so that it was not detected during analysis.

The gas composition was measured as a function of different parameters (temperature, inlet gas flow-rates, and CH_4 mole fraction in the feed). Once the mole fractions of gas species were determined, the total outlet gas flow-rate F was obtained from the Ar flow-rate (F_{Ar}) and from the outlet mole fractions (y_i) of every i-species except Ar:

$$F = F_{Ar}/(1 - \sum_i y_i) \quad (1)$$

The CH_4 conversion rate (X_{CH_4}) was then calculated as

$$X_{CH_4} = \frac{F_{0,CH_4} - F y_{CH_4}}{F_{0,CH_4}} \quad (2)$$

where F_{0,CH_4} denotes the inlet molar flow-rate of methane.

The experiments were carried out at the 1 MW solar furnace of CNRS-PROMES (Odeillo, France). The furnace is composed of a

field of 63 heliostats for full power (45 m^2 per heliostat) and of a parabolic concentrator with horizontal axis (1830 m^2, 40 m height, 54 m width) delivering up to 9000 suns (1 sun = 1 kW/m^2) at the focal plane. The solar reactor was settled at the focal point of the concentrator (18 m in front of the parabolic reflector) where high flux densities are available. During experiments, only a fraction of the parabola was used by limiting the number of heliostats tracking the sun and by using a shutter and a diaphragm. The mean solar flux density at the reactor aperture was in the range 200–300 W/cm^2 (concentration factor: 2000–3000).

3 Experimental Results

3.1 Chemical Performances at 20 kW Scale. At 20 kW scale, chemical performances were widely investigated. During one experiment, several operating conditions (flow-rates and temperature) were investigated. On the one hand, this leads to a large number of experimental data concerning chemical conversion. On the other hand, it was not possible to correlate the CB properties with the experimental conditions. Indeed, the filter was only cleaned after operating at various experimental conditions and so the CB was a mixture of products as a result of various operating parameters. These results were especially used to study the chemical performances and kinetics of the reaction [21]. The influence of the temperature and the residence time was showed to be of primary importance. In Fig. 3, the methane conversion is plotted versus the residence time for increasing temperatures between 1740 K and 2073 K. It appears that the methane conversion is enhanced when increasing temperature for a given residence time and also when increasing residence time for a given temperature. The C_2H_2 mole fraction is also reported. No clear trend appears with the temperature but it can be noted that the lowest C_2H_2 concentrations are achieved for the highest residence times. This last parameter has significant importance for decreasing the amount of the main by-product of the reaction (C_2H_2) that has a high carbon content. Temperature and residence time are critical parameters for the chemical reaction. At 50 kW scale, the influence of these two parameters on the properties of CB particles will be discussed.

3.2 Carbon Black Production at 50 kW Scale and Material Properties Assessment. Each experimental run carried out with SR50 prototype corresponds to one single experimental condition. Consequently, the CB recovered at the end in the filter corresponds to specific temperature and flow-rates. The online monitoring for one experiment at 1928 K is reported in Fig. 4 for 10.5 NL/min of CH_4 and 31.5 NL/min of Ar in the feed gas: the temperature indicated by the pyrometer pointing on a tube wall is plotted along with the temperature of a thermocouple inserted in the same tube; direct normal irradiance (DNI) and CH_4, C_2H_2, and H_2 outlet mole fractions are also reported. The methane injection period is indicated with a double arrow. It can be pointed out that this experiment was carried out with a constant DNI (960 W/m^2). After a heating period of less than 1 h, the targeted temperature is reached and methane is injected. Straight away, the hydrogen mole fraction increases. Less than 1% of CH_4 remains in the off-gas. Along the time, a slight increase of the H_2 mole fraction is observed. At the same time, the C_2H_2 concentration decreases. This is explained by a progressive carbon deposition in the tubes that leads to a higher pressure and so to a higher residence time of the gases. In addition, a catalytic reaction on the accumulated particles may occur. After 45 min, the H_2 mole fraction declines sharply because several tubes were clogged and their methane feed was stopped. The temperature given by the pyrometer is constant at about 1928 K. The one given by the thermocouple is 150 K less because the thermocouple is positioned 24 cm far from the tube entrance, so the gas is not perfectly heated and the endothermic reaction has also a cooling effect. After about 1 h of experiment, the shutter of the furnace is closed and the reactor is no longer irradiated. Consequently, the temperature decreases due to passive cooling. At the end of the experiments, the carbon black is collected and analyzed. A material balance on carbon shows that the amount of carbon recovered in the filter is 23% of the amount of carbon injected as methane in the feed. The fraction of carbon found either in the deposits in the reactor tubes or dispersed in the various components of the reactor (exit path toward the filter, unremoved deposits, and nonrecovered carbon in the filter) represents about 42% of the carbon injected. The remaining part of carbon is found as C_2H_2 in the outlet gas (35%). Concerning the material balance on hydrogen, 82% of the hydrogen contained in the fed CH_4 is found as H_2 in the outlet gas, 9% is in the form of C_2H_2, and 9% is in the form of other hydrocarbons.

Figure 5 plots the specific surface area (BET) of the samples measured by TIMCAL company (Belgium), one of the project partners. The specific surface area is one of the most important properties of a carbon black in terms of end use applications [2]. The maximum specific surface area obtained is 100 m^2/g for the test at the highest temperature and it can be observed that it decreases when decreasing the temperature for a given gas flow-rate. The higher the gas flow-rate, the lower is the specific surface area. From the BET measurements, it is possible to evaluate the mean diameter of CB particle with the following formula [2]:

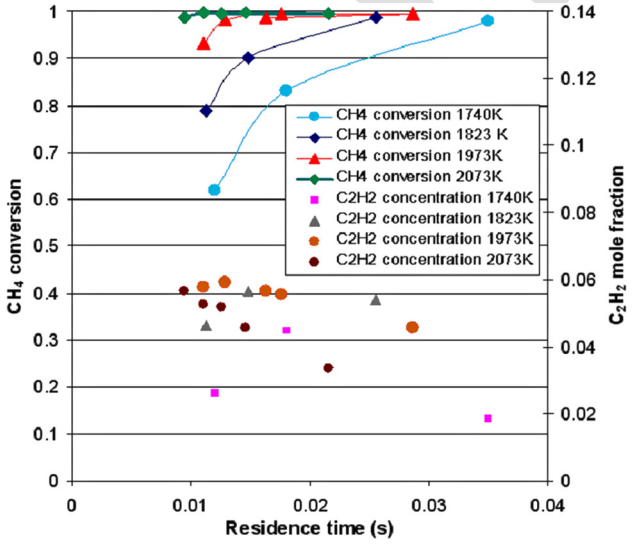

Fig. 3 CH_4 conversion and C_2H_2 off-gas mole fraction for various temperatures and residence times

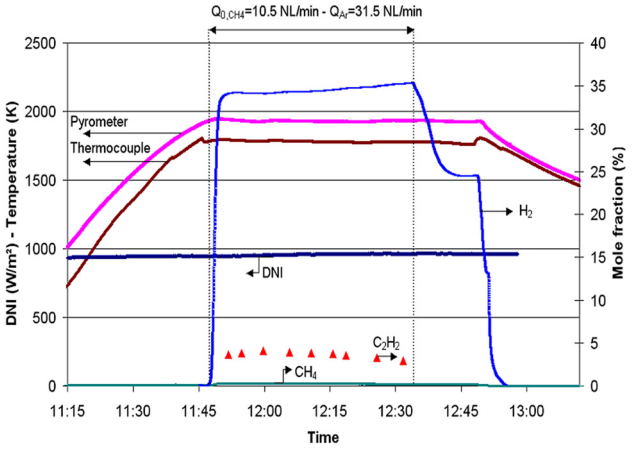

Fig. 4 Online monitoring of temperatures, DNI, H_2, C_2H_2, and CH_4 off-gas mole fractions

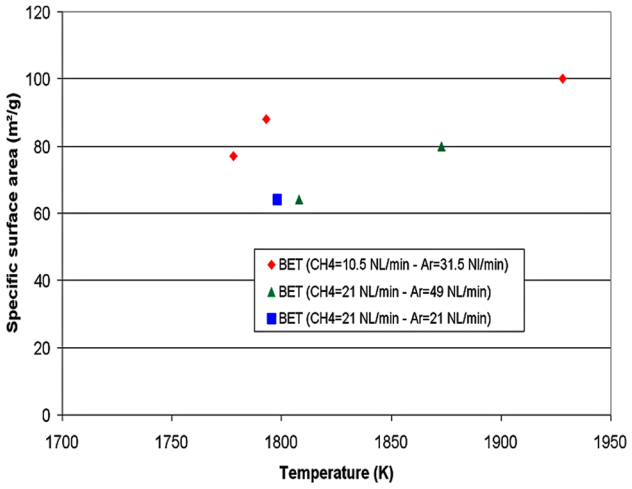

Fig. 5 Specific surface area of the carbon black particles for various experimental conditions (courtesy of TIMCAL, Belgium)

$$d_p = 6000/\rho \cdot S \quad (3)$$

S is the specific surface area (m^2/g), ρ is the density ($=2$ g/cm^3), and d_p is the mean particle diameter (nm). This formula leads to $d_p = 30$ nm for 100 m^2/g and $d_p = 50$ nm for 60 m^2/g. The mean particle diameter is ranging between these two limits. These diameters seem too high for ink-type application that requires very small particles (9–16 nm). Nevertheless, specific surface area between 60 and 100 m^2/g is found for conductive carbon black or rubber grades [22]. Microscopy analysis was also carried out via transmission electron microscopy (TEM). A shot of the sample obtained at the highest temperature (1928 K) is given in Fig. 6. The particle size distribution is between 20 and 70 nm. Nanosized particles are confirmed.

3.3 Solar Process Design and Analysis. The solar reactor experiments proved that it is possible to produce carbon black from methane decomposition with a controllable specific surface area and with possible commercial applications. As observed in Fig. 4, the reactor cannot be operated during a full sunny day without clogging. The particle deposition issue has to be addressed. Several solutions can be proposed. In order to adapt the presented solar reactor at the top of a solar tower, it was proposed to increase the gas velocity. Indeed, in the conventional furnace process for CB production, velocities up to 0.8 M are reached [2]. It was also proposed by other authors to carry out the reaction in molten metals [23], in a hot carrier gas [24], or in a fluid-wall aerosol flow reactor [10]. The thermal process [2] that consists of heating a bed (refractory-lined furnace that is fitted with a grid structure of fire bricks) in a first step and then dissociating an hydrocarbon on it in a second step could also be adapted to a solar field. However, this process is not largely used now due to its sole ability to produce large particles that have only niche applications.

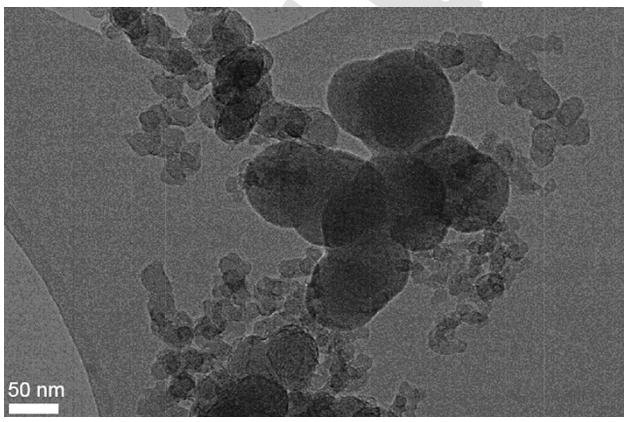

Fig. 6 TEM image of a carbon black sample obtained at 1928 K (courtesy of APTL, Greece)

The solar process for methane dissociation was designed using PROSIMPLUS3 software. The process flow diagram is shown in Fig. 7. The feed gas is composed of methane diluted with hydrogen (carrier gas) and mixed with the recycled gases (methane, acetylene, and hydrogen). The pressure of the inlet gas is fixed at 0.12 MPa to avoid any air entrance inside the process. Unconverted acetylene and methane are recycled to the solar reactor in order to produce hydrogen and carbon black only. The process is self-sufficient with respect to dilution gas because the hydrogen flow used as diluting gas is withdrawn from the produced stream. The H_2 mole fraction in the feed gas is fixed at 50%. Before entering the solar reactor, the gas mixture is first preheated at 900 °C in a heat exchanger by the gas stream exiting the solar reactor. This temperature of preheating is below the temperature of the reaction, and it is fixed accounting for the available industrial heat exchanger technologies. The solar reactor is composed of three operation units in the flow-sheet: a heat exchanger for reactants heating up to the reaction temperature (1600 °C) by solar-thermal energy, and two reactors in series to carry out the chemical reactions, $2CH_4 \rightarrow C_2H_2 + 3H_2$ ($\Delta H^\circ_1 = 188$ kJ/mol) and $C_2H_2 \rightarrow 2C + H_2$ ($\Delta H^\circ_2 = -227$ kJ/mol), respectively. A two-step mechanism is thus considered and the chemical yield of these two reactions is set at 0.9. At the solar reactor outlet, the products flow through the heat exchanger for reactants preheating before being cooled at 25 °C to allow their admittance in the filter unit. A downstream high efficiency particulate absorbing (HEPA) filter eliminates the carbon black residues. The efficiency of the filters is fixed at 99.9%. Then, the gas mixture is compressed (two-stage compression, intermediate cooling at 25 C, isentropic yield of 0.7) to reach the necessary pressure required in the pressure swing adsorption (PSA) unit (1 MPa) selected for the purification of hydrogen (yield of hydrogen recovery: 0.8). The products at the top of column are recycled to the process inlet at 0.12 MPa along with a part of pure hydrogen obtained at 0.95 MPa. In order to warrant a 50% mole fraction of hydrogen in the solar reactor, the opening of the three-way valve is controlled by the SPEC module (concentration regulation by adjustment of the valve opening). A SCRIPT is implemented to fix the solar power input in the solar reactor by adjusting the inlet methane flow-rate. A solar power of 10 MW entering the reactor is taken as a reference and a thermochemical reactor efficiency of 57% is assumed (fraction of solar power transferred to the reactants). This thermochemical efficiency is estimated assuming a blackbody receiver at 1600 °C, a concentration ratio of 3000, and accounting for 10% of conductive losses and 10% of convection losses in the reactor. The available power for the chemical reaction is thus 5.7 MW and the corresponding methane consumption is 1737 kg/h for a production of 436 kg/h of hydrogen and 1299 kg/h of carbon black. Assuming an optical efficiency of 68% for the solar concentrating system (80% for the heliostat field, 90% at the receiver aperture due to concentration defects, and 95% at the window due to reflection losses), the total power of the installation would be 14.6 MW. This power will be the basis for the economic assessment.

A sensitivity analysis was performed regarding the preheating temperature and the dilution ratio. The higher the preheating temperature, the larger the production of hydrogen and carbon black (Fig. 8). If no preheating was included, the production would be 295 kg/h of hydrogen and 877 kg/h of carbon black, which corresponds to a production decrease of more than 30% compared to the reference case (preheating at 900 °C). The influence of the preheating temperature on the production rates increases as the temperature increases (because the calorific value increases with temperature).

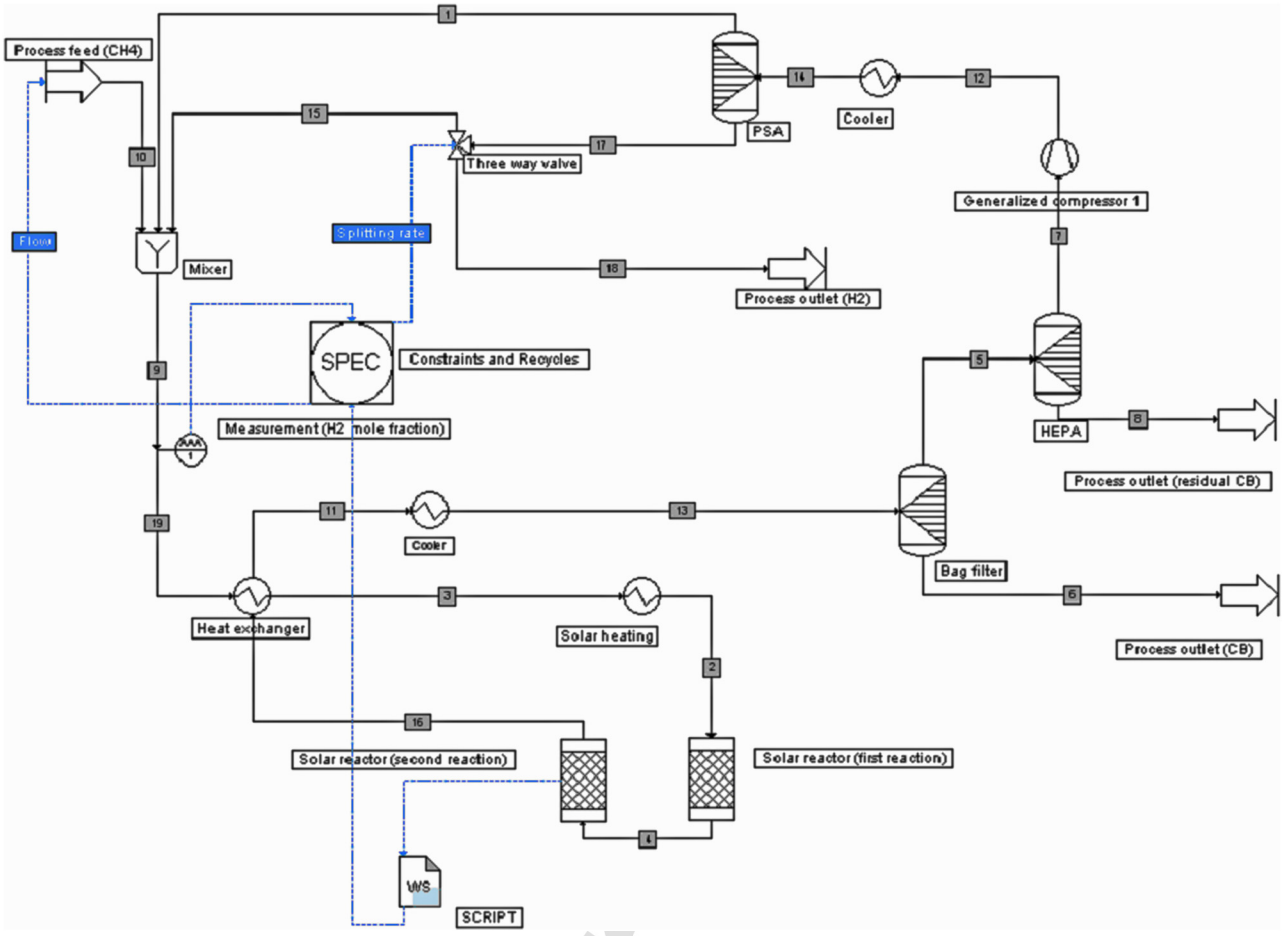

Fig. 7 Process flow-sheet for solar-thermal dissociation of methane

Increasing the dilution of methane with hydrogen reduces the process efficiency (Fig. 9). A mole fraction of H_2 below 0.3 is not considered because hydrogen is systematically recycled with the by-products at the top of the PSA column. It is not possible to get rid of this hydrogen dilution with the proposed separation method and because of the by-products recycling imposed in the flow-sheet. Indeed, although a very pure hydrogen stream is produced (99–99.99% H_2), the PSA process does not allow the complete recovery of the hydrogen contained in a gas stream (yield of H_2 recovery ranging from 60 to 90%).

An economic analysis was conducted on the basis of a model proposed by DOE (2004) [25]. The main assumptions concerning the characteristics of the chemical plant regarding the size and cost of the solar concentrating system are listed in Table 1. The hydrogen production cost from solar methane dissociation is 1.42 $/kg in the reference case (total power of the heliostat field: 14.6 MW).

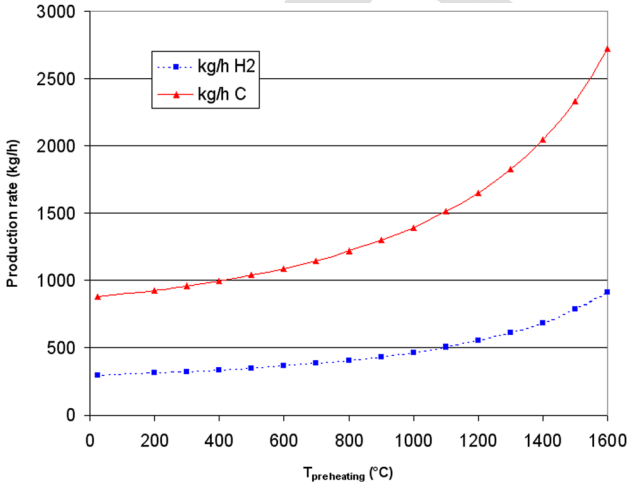

Fig. 8 Influence of the preheating temperature on the production of hydrogen and carbon black

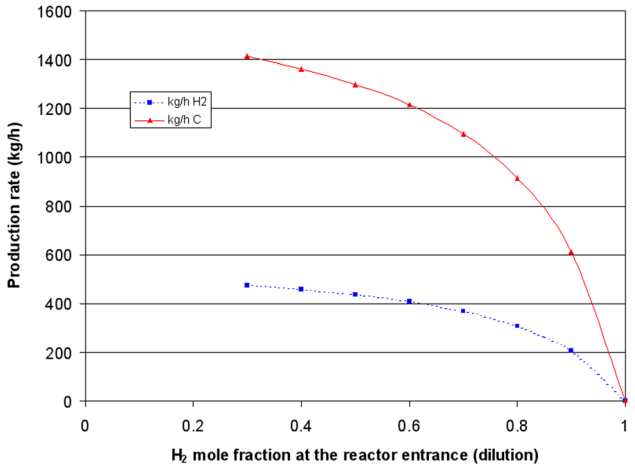

Fig. 9 Influence of the H_2 dilution on the production of hydrogen and carbon black

Table 1 Assumptions for the economic analysis in the reference case

Starting year	2030
Internal rate of return (IRR)	10%
Depreciation type	MACR
Plant life	40 yr
Inflation rate	1.90%
Effective tax rate	33% (French legislation)
Hydrogen production	436 kg/h
Annual operating hours	2000 h
Financing	100% equity financing
Construction period	2 years
Total investment	12.5 M$
Heliostats cost	200 $/m^2
Heliostats surface	17,200 m^2
(14.6 MW at a DNI of 850 W/m^2)	
Land cost	1 $/m^2
Total surface	86,000 m^2
Employees	5
Labor cost	25 $/h
Operation and maintenance costs	562,000 $
Natural gas consumption	1737 kg/h
Natural gas price	0.24 $/Nm^3
kg C/kg H_2	2.98
Carbon black selling price	0.9 $/kg
Subventions (CO_2 credits)	Not considered

The cost of hydrogen produced by methane reforming is 1.03 $/kg without CO_2 sequestration and 1.22 $/kg with CO_2 sequestration [5]. The reference cost is 1 $/kg [26] even though H_2 costs up to 2.6 $/kg were reported [27]. The cost of hydrogen from solar methane reforming is estimated to be roughly 2 $/kg [27]. Figure 10 shows the hydrogen production cost as a function of the carbon selling price (natural gas price of 0.24 $/m^3 (6$/GJ HHV) for reference year 2005). The reference case is plotted for a 10% internal rate of return (IRR) and 12.5 M$ of investment. As expected, the production cost decreases when the added value of carbon increases and the process becomes competitive with solar reforming at a carbon black selling price of 0.7 $/kg, which is a typical price of standard carbon black [28]. Besides, it is competitive with conventional reforming at a carbon black price above 1.05 $/kg. The results of the economic analysis of Dahl et al. [7] are also reported for comparison (total investment of 12.7 M$, IRR 15%, 500 kg/h H_2, 3300 h/yr), which shows moderately lower H_2 production costs because of a higher H_2 production due to a capacity factor of 0.38 against 0.23 in the present study (ratio between the number of operation hours and the total number of hours per year).

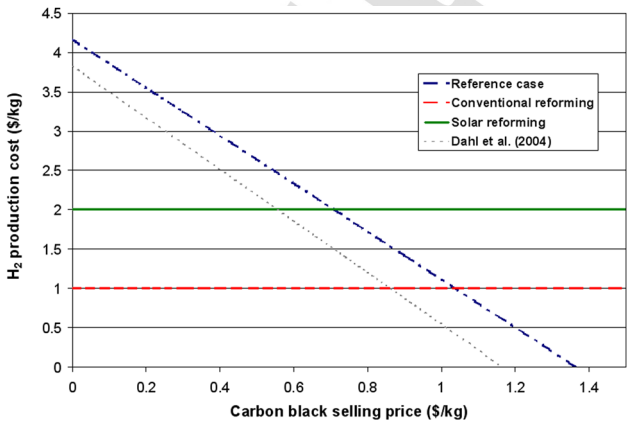

Fig. 10 H_2 production cost as a function of the carbon black selling price

4 Conclusion

Two solar chemical reactors for CH_4 dissociation were tested at the 1 MW solar furnace of CNRS-PROMES (France). SR20 was developed to study the chemical performances as functions of operating conditions. Increasing the temperature led to the methane conversion increase but increasing residence time appeared as a more efficient solution for reducing the C_2H_2 mole fraction (the main by-product) at the exit. SR50 gave information on carbon black properties. The specific surface area of the carbon particles was between 60 and 100 m^2/g, which corresponds to commercial grades. It was observed that increasing the temperature permits to increase the specific surface area and so, this provides a certain ability to the designed reactor to produce various carbon grades. Moreover, even though the gas composition at the exit will be changed, the temperature variation in a certain range will not change the hydrogen purity after the purification step (provided that it is well sized). C_2H_2 should be recirculated to reach complete conversion. Consequently, it can be concluded that varying the temperature will mainly affect the carbon black properties since hydrogen will always be produced but with more or less thermal efficiency due to the varying by-product concentrations. The main issue dealing with the methane splitting process is the particle transportation. Several options were discussed and increased gas velocities could be a solution. A process design was proposed for a 14.6 MW solar chemical plant (10 MW available at the receiver/reactor aperture) and an H_2 production cost of 1.42 $/kg was estimated for a carbon black selling price of 0.9 $/kg, which can be competitive to the conventional steam-methane reforming.

Acknowledgment

This study was funded by the European Project Solhycarb (2006–2010, Contract SES-CT2006-19770). The authors wish to thank Jean-Louis Sans, Olivier Prévost, and Marc Garrabos for their technical support during the solar reactor manufacturing and operation, and gratefully acknowledge APTL for TEM analysis and TIMCAL BE for BET measurements.

References

[1] Barreto, L., Makihira, A., and Riahi, K., 2003, "The Hydrogen Economy in the 21st Century: A Sustainable Development Scenario," Int. J. Hydrogen Energy, **28**(3), pp. 267–284.
[2] Donnet, J. B., Bansal, R. C., and Wang, M. J., 1993, *Carbon Black*, 2nd ed., revised and expanded, Science and Technology, Marcel Dekker, New York.
[3] Fabry, F., Flamant, G., and Fulcheri, L., 2001, "Carbon Black Processing by Thermal Plasma. Analysis of the Particle Formation Mechanism," Chem. Eng. Sci., **56**(6), pp. 2123–2132.
[4] Lockwood, F. C., and Van Niekerk, J. E., 1995, "Parametric Study of a Carbon Black Oil Furnace," Combust. Flame, **103**(1–2), pp. 76–90.
[5] Muradov, N., and Veziroglu, T. N., 2008, "Green Path From Fossil-based to Hydrogen Economy: An Overview of Carbon-neutral Technologies," Int. J. Hydrogen Energy, **33**, pp. 6804–6839.
[6] Ozalp, N., Kogan, A., and Epstein, M., 2009, "Solar Decomposition of Fossil Fuels as an Option for Sustainability," Int. J. Hydrogen Energy, **34**(2), pp. 710–720.
[7] Dahl, J. K., Buechler, K. J., Finley, R., Stanislaus, T., Weimer, A. W., Lewandowski, A., Bingham, C., Smeets, A., and Schneider, A., 2004, "Rapid Solar-thermal Dissociation of Natural Gas in an Aerosol Flow Reactor," Energy, **29**(5–6), pp. 715–725.
[8] Maag, G., Zanganeh, G., and Steinfeld, A., 2009, "Solar Thermal Cracking of Methane in a Particle-flow Reactor for the Co-production of Hydrogen and Carbon," Int. J. Hydrogen Energy, **34**, pp. 7676–7685.
[9] Kogan, A., Israeli, M., and Alcobi, E., 2007, "Production of Hydrogen and Carbon by Solar Thermal Methane Splitting. IV. Preliminary Simulation of a Confined Tornado Flow Configuration by Computational Fluid Dynamics," Int. J. Hydrogen Energy, **32**(18), pp. 4800–4810.
[10] Wyss, J., Martinek, J., Kerins, M., Dahl, J. K., Weimer, A., Lewandowski, A., and Bingham, C., 2007, "Rapid Solar-thermal Decarbonization of Methane in a Fluid-wall Aerosol Flow Reactor—Fundamentals and Application," Int. J. Chem. React. Eng., **5**, p. A69.
[11] Dahl, J. K., Buechler, K. J., Weimer, A. W., Lewandowski, A., and Bingham, C., 2004, "Solar-thermal Dissociation of Methane in a Fluid-wall Aerosol Flow Reactor," Int. J. Hydrogen Energy, **29**(7), pp. 725–736.
[12] Muradov, N., 2001, "Catalysis of Methane Decomposition over Elemental Carbon," Catal. Commun., **2**(3–4), pp. 89–94.

[13] Pinilla, J. L., Moliner, R., Suelves, I., Lázaro, M. J., Echegoyen, Y., and Palacios, J. M., 2007, "Production of Hydrogen and Carbon Nanofibers by Thermal Decomposition of Methane Using Metal Catalysts in a Fluidized Bed Reactor," Int. J. Hydrogen Energy, **32**(18), pp. 4821–4829.

[14] Wullenkord, M., Funken, K. H., Sattler, C., and Pitz-Paal, R., 2010, "Hydrogen Production by Thermal Cracking of Methane—Investigation of Reaction conditions," *Proceedings of WHEC 2010*, Essen, Germany.

[15] Abanades, S., Tescari, S., Rodat, S., and Flamant, G., 2009, "Natural Gas Pyrolysis in Double-walled Reactor Tubes Using Plasma Arc or Concentrated Solar Radiation as External Heating Source," J. Nat. Gas Chem., **18**(1), pp. 1–8.

[16] Lynum, S., Hox, K., Haugsten, K., and Langoy, J., 1993, "System for the Production of Carbon Black," Kvaerner Eng., Patent WO 93/20153.

[17] Boutot, T. J., Buckle, K., Collins, F. X., Claus, S. J., Estey, C. A., Fraser, D. M., Liu, Z., and Whidden, T. K., 2007, "Decomposition of Natural Gas or Methane Using Cold Arc Discharge," Atlantic Hydrogen, Patent WO2007/019664 A1.

[18] Rodat, S., Abanades, S., Sans, J. L., and Flamant, G., 2009, "Hydrogen Production From Solar Thermal Dissociation of Natural Gas: Development of a 10 kW Solar Chemical Reactor Prototype," Solar Energy, **83**(9), pp. 1599–1610.

[19] Rodat, S., Abanades, S., and Flamant, G., 2009, "High-Temperature Solar Methane Dissociation in a Multitubular Cavity-Type Reactor in the Temperature Range 1823–2073 K," Energy Fuels, **23**, pp. 2666–2674.

[20] Rodat, S., Abanades, S., Sans, J. L., and Flamant, G., 2010, "A Pilot-scale Solar Reactor for the Production of Hydrogen and Carbon Black From Methane Splitting," Int. J. Hydrogen Energy, **35**(15), pp. 7748–7758.

[21] Rodat, S., Abanades, S., Coulié, J., and Flamant, G., 2009, "Kinetic Modelling of Methane Decomposition in a Tubular Solar Reactor," Chem. Eng. J., **146**(1), pp. 120–127.

[22] Parkash, S., *Petroleum Fuels Manufacturing Handbook* (McGraw Hill Professional, 2009).

[23] Serban, M., Lewis, M. A., Marshall, C. L., and Doctor, R. D., 2003, "Hydrogen Production by Direct Contact Pyrolysis of Natural Gas," Energy Fuels, **17**, pp. 705–713.

[24] Shpilrain, E. E., Shterenberg, V. Y., and Zaichenko, V. M., 1999, "Comparative Analysis of Different Natural Gas Pyrolysis Methods," Int. J. Hydrogen Energy, **24**(7), pp. 613–624.

[25] DOE, 2004, DOE Spreadsheet download at http://www.hydrogen.energy.gov//h2a_production.html.

[26] Perkins, C., and Weimer, A. W., 2009, "Solar Thermal Production of Renewable Hydrogen," AIChE J., **55**(2), pp. 286–293.

[27] Pregger, T., Graf, D., Krewitt, W., Sattler, C., Roeb, M., and Moller, S., 2009, "Prospects of Solar Thermal Hydrogen Production Processes," Int. J. Hydrogen Energy, **34**(10), pp. 4256–4267.

[28] Adams, R., 2007, "Booming World Carbon Black Demand but Price Rises Fail to Keep Pace With Rising Gas and Feedstock Costs," Focus Pigm., **3**, pp. 1–2.

AQ1

AQ1: Please provide the location of the publisher for Ref. 22.